Journal of Advanced Research in Fluid Mechanics and Thermal Sciences

Journal homepage:
https://semarakilmu.com.my/journals/index.php/fluid_mechanics_thermal_sciences/index
ISSN: 2289-7879

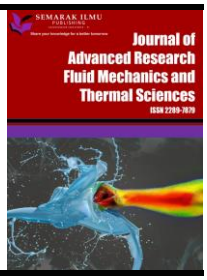

Rayleigh-Benard Convection Inside Square Cavities Filled with Thermodependent Non-Newtonian Fluids and Subjected to External Magnetic Field

Nouri Redouane[1,*], Mourad Kaddiri[1], Youssef Tizakast[1], Hamza Daghab[1]

[1] Industrial Engineering and Surface Engineering Laboratory, FST, Sultan Moulay Slimane University Beni-Mellal, Morocco

ARTICLE INFO

Article history:
Received 15 July 2023
Received in revised form 2 October 2023
Accepted 13 October 2023
Available online 25 October 2023

Keywords:
Natural convection; Rayleigh-Benard; non-Newtonian fluid; magnetic field; power law; temperature dependence on viscosity

ABSTRACT

The aim of this study is to numerically evaluate the Rayleigh-Benard natural convection magnetohydrodynamic (MHD) of a non-Newtonian fluid along a square cavity whose viscosity depends on the temperature. The rheological behavior of the fluids under consideration is represented using the Ostwald-De-Weale power law. Subsequently, the dominant equations are transformed into a non-dimensional form and computed using the finite volume method (FVM). The literature was used to validate the model, and excellent agreement was achieved by varying the fluid characteristics with Prandtl numbers Pr, Hartmann numbers, Ha, Rayleigh numbers, Ra, the behavior index, n, and inclination angle, Θ. The numerical results are discussed in terms of velocity, mean Nusselt number Nu, maximum current function $|\Psi_{max}|$, streamlines, and isotherms. The study finds that the onset of convection is delayed with increasing values of n and Ha. Additionally, it revealed that the flow intensity and heat transfer decrease as the Hartmann number rises for both Newtonian and non-Newtonian fluids. At very high Ha values, the heat transfer is mainly assured by the conduction regime. Moreover, the temperature-dependent viscosity in MHD results in the disappearance of the Centro symmetry of the central cell and the migration of the center towards the active wall.

1. Introduction

The free convection of fluids under the influence of a magnetic field, known by the scientific term magnetohydrodynamics (MHD), is a discipline that has a vast variety of applications in engineering as well as in nature, such as cooling electronic components, nuclear reactors, and the process of manufacturing materials crystal growth [1-3]. MHD (magnetohydrodynamics) plays a crucial role in the biomedical field, including applications such as reducing tissue temperature, separating and treating cancerous tumors, aiding in vehicles and drug delivery, as well as in energy storage, building, conservation, firefighting, and the production of chemical, food, and metallurgical products [4-7]. This is the reason why magnetohydrodynamics is a very important research subject.

* *Corresponding author.*
E-mail address: redouane.nouri@usms.ma

https://doi.org/10.37934/arfmts.110.2.138156

Before initiating the problematic research on MHD, extensive studies demonstrated the occurrence of free convection under the influence of a magnetic field across various fluid types and boundary conditions (Dirichlet, Neumann) in both square and rectangular cavities. Research on free convection with Newtonian fluids under the impact of a magnetic field has been conducted for both horizontal thermal conditions in published papers by Oreper and Szekely [8], Pirmohammadi and Ghassemi [9], Ghasemi *et al.,* [10], Kefayati [11], and Alchaar *et al.,* [12] and vertical thermal conditions in other published scientific articles by Liao *et al.,* [13], Benzema *et al.,* [14], Zürner *et al.,* [15], and Chtaibi *et al.,* [16]. The flow of conductive fluids during natural convection is notably affected by the interaction between the magnetic force and buoyancy forces, contributing to flow stabilization and the regulation of oscillatory instabilities. Considering the prevalence of non-Newtonian rheological fluids in industrial installations, there has been a significant focus from researchers on studying MHD with this type of fluid. Notably, among the authors who have conducted research on MHD with horizontal thermal conditions and non-Newtonian fluids we find the published papers by Kefayati [17], Dimitrienko and Li [18], and Makayssi *et al.,* [19], while Liao *et al.,* [13] focused on Newtonian fluids while also accounting for the mass transfer. The results highlight the considerable impact of magnetic field alignment on streamlines and isotherms within a square cavity. They demonstrate that both the average Nusselt number and the maximum flux intensity decrease as the magnetic field strength increases. Furthermore, a decrease in the behavior index n leads to a significant rise in fluid circulation intensity and heat transfer. However, the influence of n becomes less pronounced for high values of Ha, particularly in the presence of strong magnetic fields. Chtaibi *et al.,* [16] presented a preliminary study obtained from numerical simulations of free convection in a square enclosure of the Rayleigh-Benard type filled with a ferrofluid under the impact of an outside magnetic field. The equations describing the physical problem were solved using Boltzmann method. These results show that increasing the Hartmann number brought the ferrofluid flux back to the resting state from a certain threshold value which depends on Ra. Moreover, in addition to the intensity of the magnetic field, its direction is also a parameter which plays a non-negligible role. Naffouti *et al.,* [20] carried out a study on the direction of the magnetic field imposed on the flow structure and the rate of heat transfer in a cubic enclosure heated from below they noticed that the presence of magnetic field results in the distortion of the forms iso surfaces not only in the center of the cavity but also in the vicinity of each side. And that the effect of the magnetic field greatly decreases the rate of heat transfer. In fact, the average profile of the Nusselt number presents two peaks which may be due to the local appearance of instabilities and bifurcation phenomena. It is also obvious that the direction of the magnetic force can help or oppose the buoyant force. Ahmed *et al.,* [21] studied the impact of the magnetic field on Rayleigh Benard convection in a closed square enclosure which was analyzed by LBM (Lattice Boltzmann Method). Heat transfer applications and flow characteristics inside the closed cavity are largely dependent on magnetic field strengths, tilt angles, and Ra values. Heat transport is shown to degrade with an increase in Ha value at various Ra and Pr values. For a low Ra value, the magnetic field has little effect, because the isotherms begin to intersect one another in parallel due to surpassing of RB convection, and conduction mostly dominates the heat transfer inside the container, isotherms become parallel for $Ha > 25$, at $Ra = 10^5$ to 10^6, but Higher levels of the buoyancy parameter created instability and oscillation, making this characteristic invisible. They also observed that for various fluids, the Ha numbers significantly affect the Nu value. Benzema *et al.,* [14] conducted a numerical study to demonstrate how the orientation of the magnetic field influences the Rayleigh-Benard convection of a nanofluid in a square enclosure. Empirical models were employed to simulate the nanoparticle presence in the fluid. The study revealed a direct correlation between the Hartmann number and the average Nusselt number, indicating that the introduction of nanoparticles enhances heat transfer

only in the presence of a magnetic field. Makayssi *et al.,* [22] numerically studied the impact of an ascending magnetic field on thermally driven convection in a square enclosure subjected to a vertical thermal gradient and the normal walls are assumed to be insulated. For all values of Hartmann and behavior indices, there are several cells in the flow, and the number of cells relies on the Hartmann number rather than the behavior index. A rise in Ha causes the intensity of flow and heat transfer to decrease for all values of n, Additionally, for dilating fluids at extremely high values of Ha, convection goes towards a conduction regime, but for pseudoplastic fluids, it is delayed. A crucial value Rac of the Rayleigh number, which relies on both Hartmann and the behavior index, controls the beginning of convection.

However, it is important to note that in the majority of investigations, the characteristics of fluids are generally considered to be stable despite temperature fluctuations. But this only applies to a limited temperature variation between thermally active surfaces. For many fluids, the change in viscosity with temperature is often much higher than for other properties. Among the works that show this dependence, we find Hirayama and Takaki [23] and Kaddiri *et al.,* [24]. However, there is no research on Rayleigh Benard convection in a square cavity exposed to a magnetic field for a non-Newtonian fluid whose viscosity varies with temperature.

To address the scarcity of studies concerning the square cavity exposed to a vertical flow and a magnetic field for non-Newtonian fluids with temperature-dependent viscosity, the research will concentrate on analyzing the flow structure, its intensity, and the heat transfer characteristics for non-Newtonian Rayleigh-Bénard fluids under the influence of a magnetic field.

2. Methodology

2.1 Formulation of the Problem and Viscosity Model

Figure 1 depicts a two-dimensional square enclosure of dimensions (H', H'), subject to a uniform external magnetic field $\overrightarrow{B_0}$. The enclosure experiences a flow directed by its horizontal walls, while the adiabatic conditions are maintained along the normal walls.

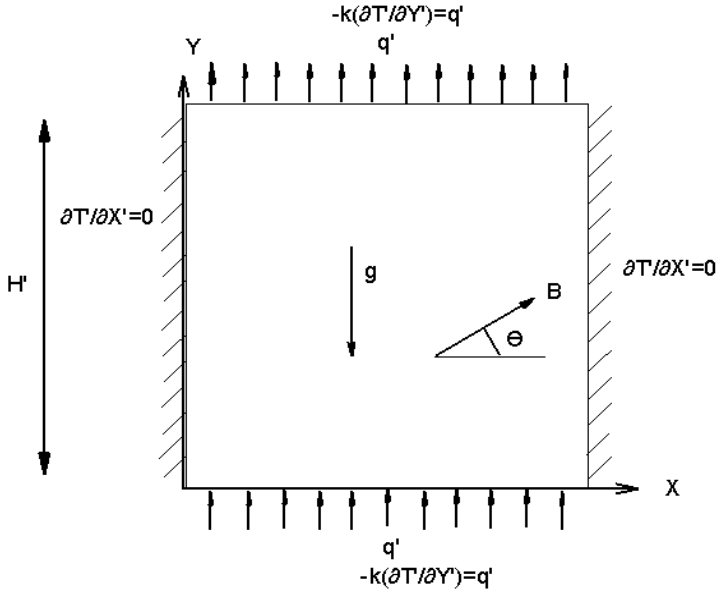

Fig. 1. Cavities with applied heat conditions and magnetic fields are shown schematically with the corresponding markers

Non-Newtonian electrically conductive fluids whose rheological behavior can be modeled using Ostwald-de Wael power law model and which, in terms of apparent viscosity, vary with temperature may be stated as:

$$\mu_a{}' = K_T \left\{ 2\left[\left(\frac{\partial U\prime}{\partial X\prime}\right)^2 + \left(\frac{\partial V\prime}{\partial Y\prime}\right)^2 \right] + \left(\frac{\partial U\prime}{\partial Y\prime} + \frac{\partial V\prime}{\partial X\prime}\right)^2 \right\}^{\frac{n_k-1}{2}} \tag{1}$$

where n_k represents the behavior of the flow, and k_T represents the consistency index and which are generally temperature dependent, However, the change of n as a function of temperature is negligible. (nk≈constant = n) with respect to that of k_T, this may be calculated using the Frank-Kamenetskii exponential rule [24]:

$$K_T = \mathrm{k}e^{-\mathrm{b}(T'^2 - T_r'^2)}$$

where b, also known as the thermal dependence coefficient, is an exponent connected to the flow energy activation and the universal gas constant. k is the consistency index at the reference temperature Tr. For $n = 1$ Newtonian behavior is seen, and consistency is just the viscosity $\mu_a = \mathrm{k}$. For $0 < n < 1$, as the shear rate increases, the effective viscosity diminishes. And the behavior is shear thinning (or pseudo plastic). And for $n > 1$, the behavior is shear-thickening (or dilatant), and the viscosity rises with the shear rate.

2.2 Equations and Boundary Conditions

The dimensionless parameters employed in this context are:

$(X,Y) = (X',Y') / H'$, $(U,V) = (U',V') / (\alpha / H')$, $T = (T') / (q'H' / \lambda)$, $P = P'/(\rho\alpha^2/H'^2)$ and $\Psi = \Psi'/\alpha$.

For this reason, the controlling equations without dimension are given as follows:

Continuity Equation

$$\frac{\partial U}{\partial X} + \frac{\partial V}{\partial Y} = 0 \tag{2}$$

Momentum Equation

$$U\frac{\partial U}{\partial X} + V\frac{\partial U}{\partial Y} = -\frac{\partial P}{\partial X} + Pr\begin{bmatrix} 2\frac{\partial \mathfrak{u}_a}{\partial x}\frac{\partial U}{\partial X} + \frac{\partial \mathfrak{u}_a}{\partial Y}\left(\frac{\partial V}{\partial X} + \frac{\partial U}{\partial Y}\right) \\ +\mathfrak{u}_a\left(\frac{\partial^2 U}{\partial Y^2} + \frac{\partial^2 U}{\partial X^2}\right) \end{bmatrix} + Ha^2 Pr\, sin\,\Theta \begin{pmatrix} V\, cos\,\Theta \\ -U\, sin\,\Theta \end{pmatrix} \tag{3}$$

$$U\frac{\partial V}{\partial X} + V\frac{\partial V}{\partial Y} = -\frac{\partial P}{\partial Y} + Pr\begin{bmatrix} 2\frac{\partial \mathfrak{u}_a}{\partial Y}\frac{\partial V}{\partial Y} + \frac{\partial \mathfrak{u}_a}{\partial X}\left(\frac{\partial U}{\partial Y} + \frac{\partial V}{\partial X}\right) \\ +\mathfrak{u}_a\left(\frac{\partial^2 V}{\partial X^2} + \frac{\partial^2 V}{\partial Y^2}\right) + RaT \end{bmatrix} + Ha^2 Pr\, cos\,\Theta \begin{pmatrix} U\, sin\,\Theta \\ -V\, cos\,\Theta \end{pmatrix} \tag{4}$$

Energy Equation

$$U\frac{\partial T}{\partial X}+V\frac{\partial T}{\partial Y}=\frac{\partial^2 T}{\partial X^2}\ +\frac{\partial^2 T}{\partial Y^2} \tag{5}$$

with

$$\mu_a=e^{-mT}\left\{2\left[\left(\frac{\partial U}{\partial X}\right)^2+\left(\frac{\partial V}{\partial Y}\right)^2\right]+\left(\frac{\partial U}{\partial Y}+\frac{\partial V}{\partial X}\right)^2\right\}^{\frac{n-1}{2}} \tag{6}$$

The current function Ψ is used to study the flux structure:

$$U=\frac{\partial \Psi}{\partial X}\quad ;\quad V=-\frac{\partial \Psi}{\partial Y} \tag{7}$$

Dominant Parameters

Furthermore, to the flow behavior index, four other significant factors without units are present in the determining formulae. These factors are the Rayleigh, Prandtl, Pearson and Harman numbers calculated as follows:

$$Ra=\frac{g\beta H'^{(2+2n)}q'}{(K/\rho)\alpha^n\lambda}\quad ;\quad Pr=\frac{(K/\rho)H'^{(2-2n)}}{\alpha^{2-n}};\ m=-\frac{1}{K_T}\frac{dK_T}{dT}=-\frac{dln\left(\frac{K_T}{K}\right)}{dT}\ ;\ Ha=B_0'H'^n\left(\frac{\sigma}{k}\alpha^{1-n}\right)^{\frac{1}{2}} \tag{8}$$

The Pearson number m evaluates the impact of temperature variation on apparent viscosity. This is a new quantity that is taken into account in this analysis. In the concrete context, the non-dimensional parameters of the corresponding limits are:

$$U=V=\Psi=\frac{\partial T}{\partial Y}+1=0\ \ For\ Y=0\ and\ Y=1$$

and

$$U=V=\Psi=\frac{\partial T}{\partial X}=0\ \ For\ X=0\ and\ X=1 \tag{9}$$

2.3 Heat Transfer

The formula shown below is utilized to calculate the average Nusselt number, which measures the natural convection flux contribution to the overall heat transfer:

$$Nu=\int_0^1\frac{1}{\Delta T_h}dX \tag{10}$$

with, ΔT_{h} is the temperature difference between the two horizontal walls.

2.4 Numeric

Previous Eq. (2) to Eq. (5) associated with boundary conditions Eq. (9) can be expressed generally as follows [11]:

$$\frac{\partial}{\partial X}\left(U\emptyset - \Gamma\frac{\partial\emptyset}{\partial X}\right) + \frac{\partial}{\partial Y}\left(V\emptyset - \Gamma\frac{\partial\emptyset}{\partial Y}\right) = S_{\emptyset} \quad (11)$$

with $\emptyset$ the variable which can be either T, U or V, to find the equation of quantity of motion Γ is replaced by $\mathrm{Pr}\mu_a$, and for the energy it is 1, and $S_{\emptyset}$ is the source term. The Eq. (12) must be converted into a linear system that results in:

$$A_P\emptyset_P = A_W\emptyset_W + A_E\emptyset_E + A_S\emptyset_S + A_N\emptyset_N + S_{\emptyset} \quad (12)$$

with $\emptyset_P$ are variables U, V and T at point P and Eq. (12) is the final version of the discretized equation relating the variable to its nearby grid point. ΔV = ΔX x ΔY where ΔX and ΔY are the pitch of the X and Y directions. With the use of the line-by-line method based on the tridiagonal matrix algorithm (TDMA), the discretized system created for control volume is composed of a series of linear algebra equations that are then simply resolved [25-27]. The SIMPLE method resolves the velocity-pressure relationship [28]. The numerical code is implemented using Fortran and the solution convergence is obtained when the maximum residual of all the governing equations is less than 10^{-6}.

$$MAX\left(\frac{(\emptyset)^{n+1}-(\emptyset)^{n}}{(\emptyset)^{n+1}}\right) \leq (10)^{-6} \quad (13)$$

2.5 Validation of the Numerical Code Findings Used

Table 1 compares the numerical findings for both Newtonian and non-Newtonian fluids with the results from Turan *et al.,* [29]. The considered geometry is a square submitted to imposed constant temperatures on the vertical walls. Table 2 and Table 3 provide comparisons in a similar configuration but this time in the presence of the magnetic field with references of Makayssi *et al.,* [19] and Pirmohammadi *et al.,* [30] respectively. The three tables confirm the excellent agreement with all comparisons indicating that the highest error does not exceed 1.25% testifying of the current numerical code accuracy.

Table 1
The values numerical results at $Ra = 10^4$ for different value of n and $Pr = 100$

	Present Works				Turan *et al.,* [29]	
	Nu	Dev (%)	UMAX	Dev (%)	Nu	UMAX
n=1.8	1.030	0	1.575	0.38	1.030	1.569
n=1	2.123	0.09	14.361	0.13	2.121	14.342
n=0.6	3.472	0.02	42.135	0.05	3.471	42.157

Table 2
Numerical results at results at $Ha = 30$, Θ= 0°, $n = 1$, and various values of Ra

	$\lvert\Psi_{max}\rvert$			**Nu**			Dev (%)
$\boldsymbol{Ra}$	Present study	Makayssi *et al.,* [19]	Pirmohammadi *et al.,* [30]	Present study	Makayssi *et al.,* [19]	Pirmohammadi *et al.,* [30]	Present study
$\mathbf{10^3}$	0.127	0.128	0.128	1.001	1	1.002	0.78
$\mathbf{10^4}$	1.193	1.192	1.193	1.175	1.175	1.183	0.68
$\mathbf{10^5}$	5.716	5.698	5.710	3.121	3.132	3.151	0.31
$\mathbf{10^6}$	14.149	14.088	14.088	7.943	7.899	7.907	0.96

Table 3
Numerical results at $Ra = 10^5$, Θ= 0°, $n = 1$, and for different values of Ha

	$\|\Psi_{max}\|$			Nu			Dev (%)
Ha	Present study	Makayssi *et al.,* [19]	Turan *et al.,* [29]	Present study	Makayssi *et al.,* [19]	Turan *et al.,* [29]	Present study
0	11.194	11.177	11.053	4.712	4.713	4.738	1.25
15	8.525	8.498	8.484	4.114	4.121	4.143	0.70
30	5.716	5.698	5.710	3.121	3.132	3.150	0.92
45	3.829	3.818	3.825	2.344	2.355	2.369	1.06
60	2.627	2.621	2.623	1.831	1.840	1.851	1.09

2.6 Grid Size

Table 4 studies the stability of the results as a function of the number of grid points to choose a mesh size that leads to better accuracy and optimal computation time The results obtained for $Ra = 10^4, n = 0.6$, $\Theta = 0°$ and $Ha = 10$ show that the 120*120 grid is sufficient to accurately simulate the problem at hand.

Table 4
Maximum Stream function $|\Psi_{max}|$ and Nusselt number $\overline{Nu}$ inside the enclosure for different mesh sizes at $Ra = 10^4$, $n = 0.6$, $theta = 0$ and $Ha = 10$

Grids	$\overline{\mathrm{Nu}}$	Dev (%)	$\|\Psi_{\max}\|$	Dev (%)
80×80	2.509	-----	4.230	-----
120×120	2.507	0.07	4.230	0
200×200	2.505	0.07	4.227	0.07
300×300	2.500	0.19	4.226	0.02

3. Results

In this part, the results are presented and discussed according to the previously established dimensionless parameters, namely the Prandtl number, Pr, the Pearson number, m, $0 \leq m \leq 10$, the Hartmann number, Ha, the behavior index flow rate, n, which varies in the range $0{,}6 \leq n \leq 1{,}4$ and the Rayleigh number, Ra. Initially, in order to prevent difficult scenarios caused by instability and bifurcations, proper study parameters were chosen. Table 5 presents the effect of Pr for Newtonian and non-Newtonian fluids considered in this study, from the analysis of the table it can be clearly drawn that any increase in Pr from 60 no longer has effect on $|\Psi_{max}|$ and Nu. Therefore, this work adopts numerical simulations with $Pr = 100$, Lamsaadi *et al.,* [31] showed that this fact is true even when there is no magnetic field.

Table 5
Effect of the Prandtl number

n	Pr	Ha=20		Ha=40		Ha=60	
		$\|\Psi max\|$	Nu	$\|\Psi max\|$	Nu	$\|\Psi max\|$	Nu
0.6	1	7.27	3.76	3.3	3.06	1.86	2
	20	6.96	4.19	3.28	3.13	1.86	2.01
	60	6.95	4.20	3.28	3.13	1.86	2.01
	100	6.95	4.20	3.28	3.13	1.86	2.01
1	1	6.53	2.82	3.26	2.32	1.79	1.69
	20	6.53	2.85	3.26	2.32	1.79	1.69
	60	6.53	2.85	3.26	2.32	1.79	1.69
	100	6.53	2.85	3.26	2.32	1.79	1.69
1.4	1	2.82	2.14	2.32	1.76	1.69	1.4
	20	2.85	2.14	2.32	1.76	1.69	1.4
	60	2.85	2.14	2.32	1.76	1.69	1.4
	100	2.85	2.14	2.32	1.76	1.69	1.4

Figure 2 displays the variation of the critical number of Rayleigh, Rac, that is to say, the threshold of appearance of the convection, according to the n for various values of Ha, we note that for any value of Ha, Rac is a raising function of n, which means that shear-thinning behavior anticipates convection, whereas shear-thickening has the opposite result. We see that, for a given n, a rise in Ha leads to an increase in Rac, expressing the fact that the MHD tends to eliminate convection. However, the optimal Rayleigh value for studying Rayleigh Benard convection in interaction with the magnetic field is $Ra = 10^5$.

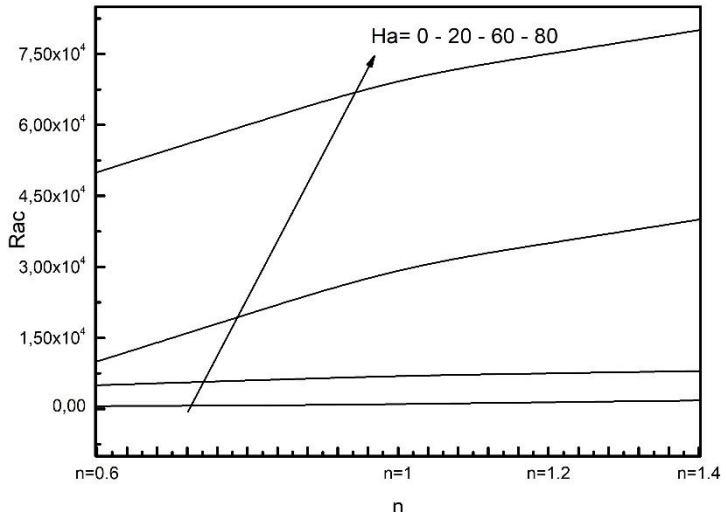

Fig. 2. Evolution of Rac with n, for various values of Ha

Figure 3 and Figure 4 show the streamlines and isotherms for $Ra = 10^5$, $\Theta = 0°$, and different values of Ha. It is evident that a rise in Ha causes major qualitative and quantitative changes in the intensity and the flow structure in the convective regime in the presence of the magnetic field. For a given value of n, the more Ha increases, the more the streamlines tilt, and this is due to the influence of the magnetic force, which modifies the trajectory of the convective movement of the fluid. The greatest qualitative changes are observed in the central region of the cavity. In fact, the central cells are horizontal for $Ha = 0$, which take an oval shape for $Ha = 60$ and straighten until approaching the vertical shape for $Ha = 100$, and by soot, it has become more and more tight next to the vertical walls, this change is significant when the power law index is decreased, the quantitative changes is

very intense because the flow intensity is reduced significantly from 36 to 0.1 when the number Ha further increases up to $Ha = 100$. Overall, the influence of the magnetic force is contrary to that of the buoyancy force, this demonstrates that the coupling of Rayleigh Benard convection and the magnetic field reinforces the flow braking phenomena.

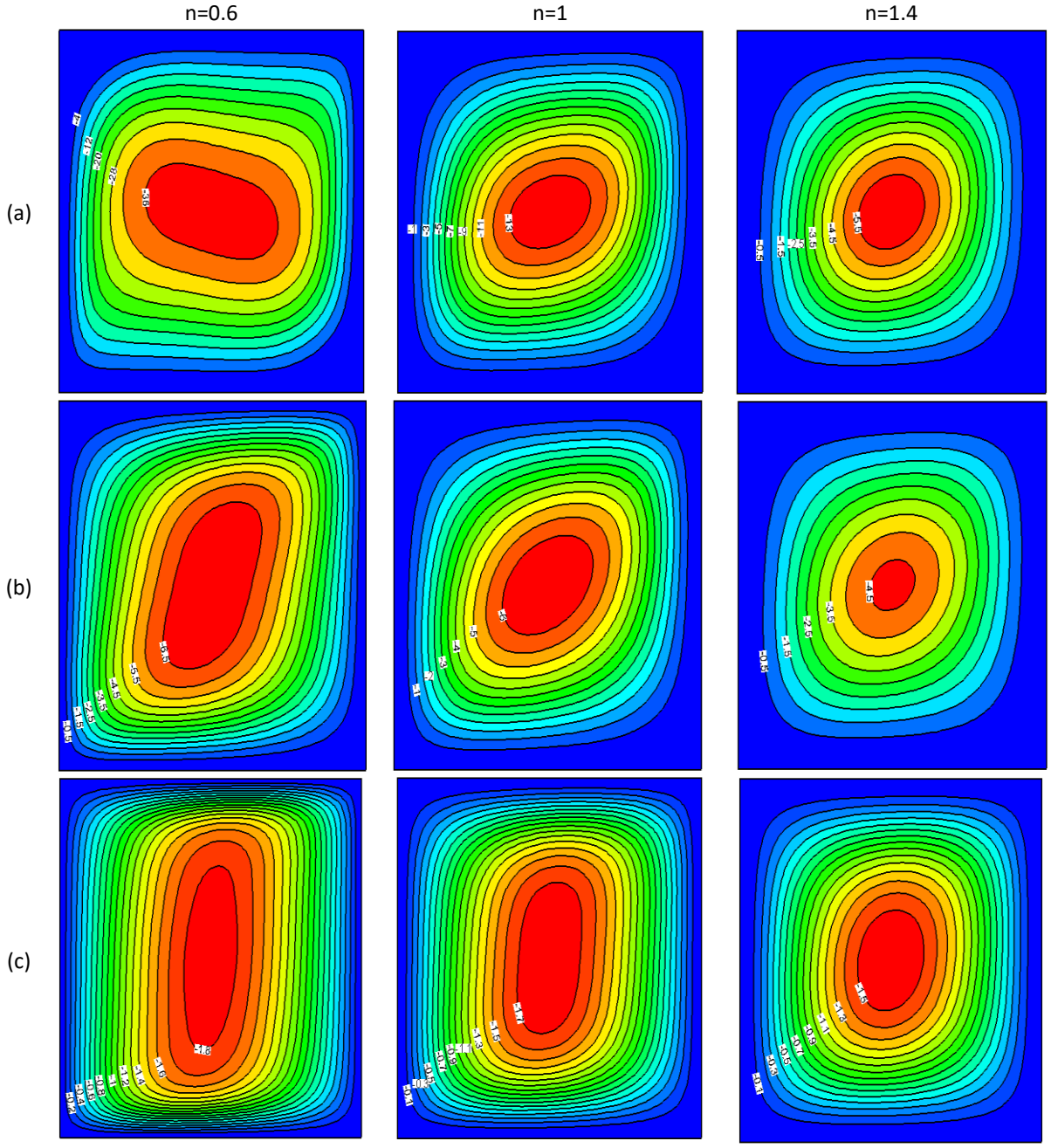

(d)

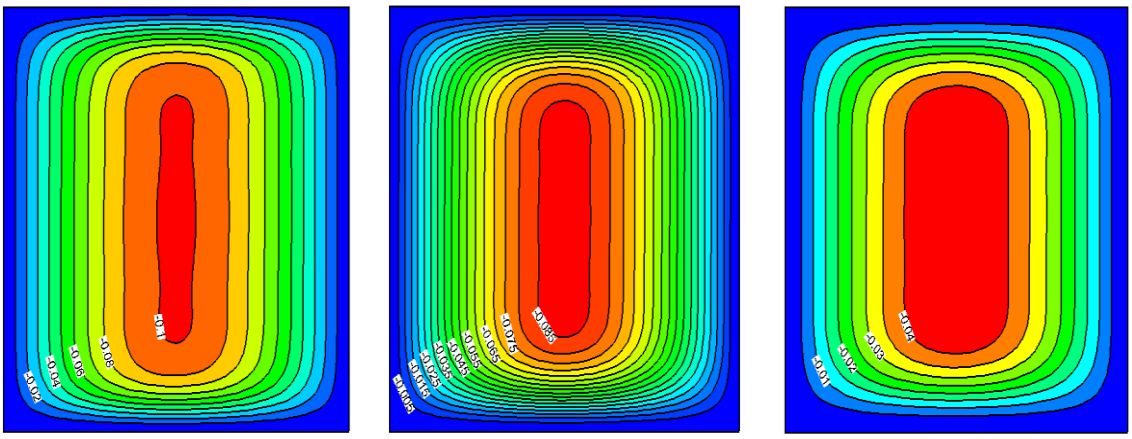

Fig. 3. Streamlines for $Ra = 10^5$, $\Theta = 0^{\circ}$, for different values of n ((left) n =0.6, (middle) n =1, (right) n =1.4) and various values of Ha ((a) (Ha=0) 0, (b) (Ha= 20), (c) (Ha=60), (d) (Ha=100))

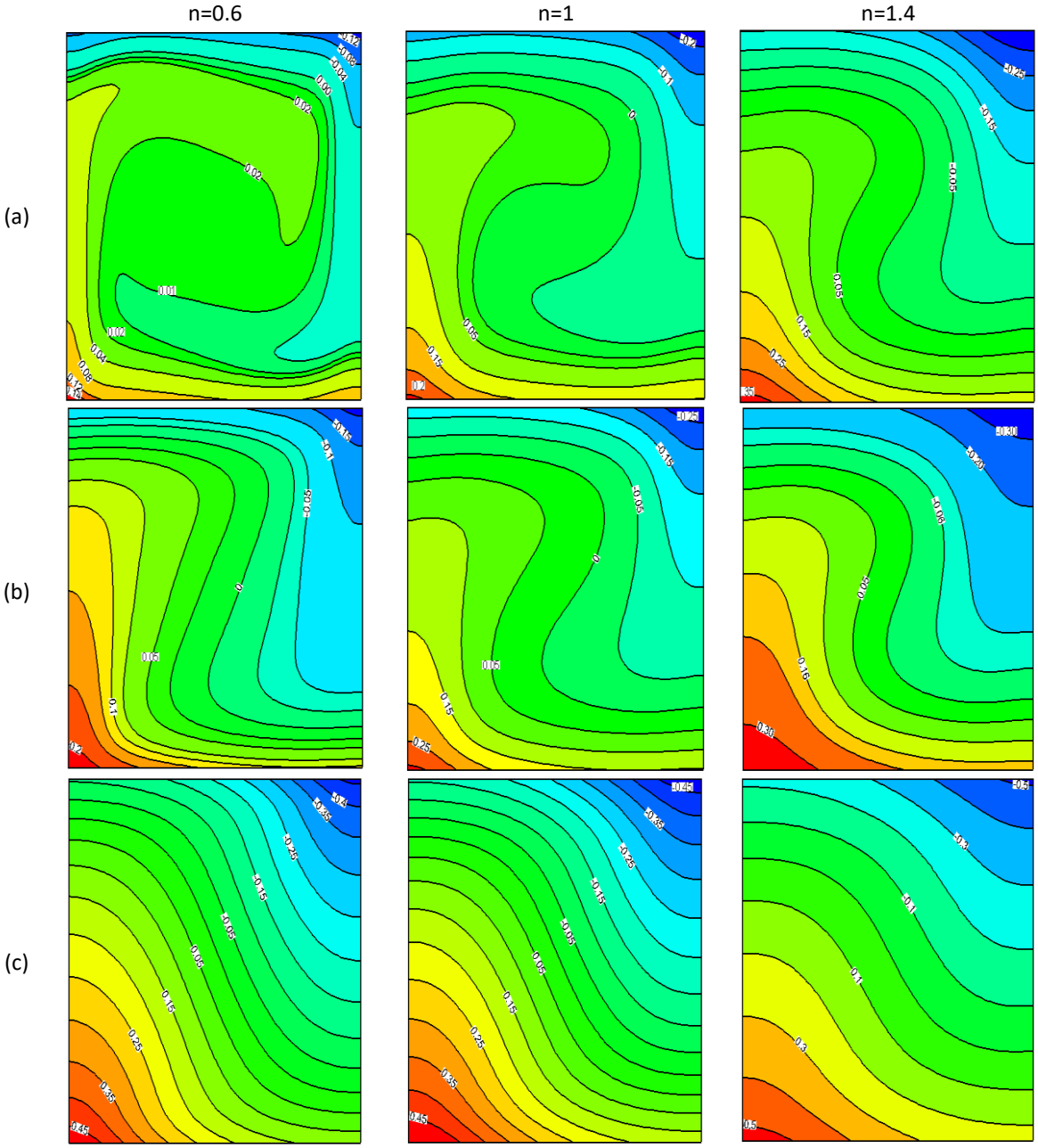

(d)

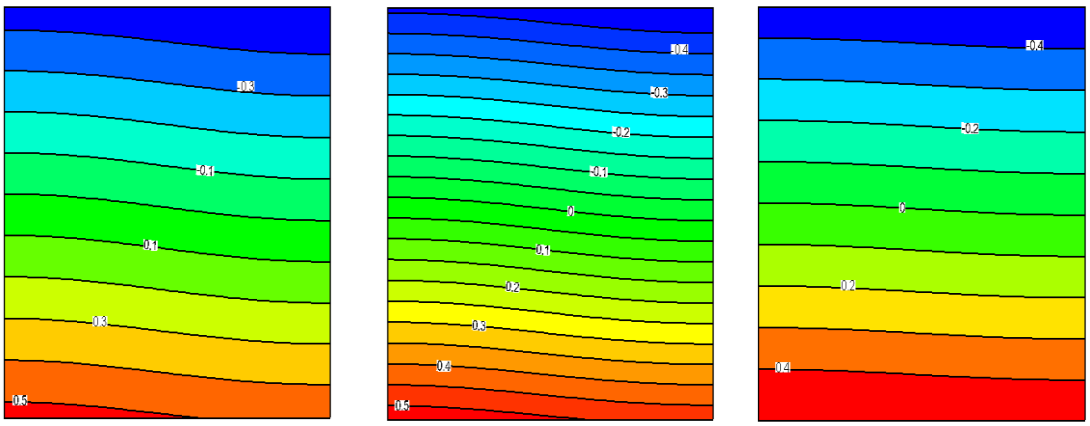

Fig. 4. Isotherms for $Ra = 10^5$, $\Theta = 0^{\circ}$,for different values of n ((left) n =0.6, (middle) n =1, (right) n =1.4) and various values of Ha ((a) (Ha=0) 0, (b) (Ha= 20), (c) (Ha=60), (d) (Ha=100))

Due to the strong coupling between the velocity and temperature fields, the qualitative and quantitative effects on the temperature distribution inside the cavity, accompanying the increase in the Hartmann number as can be seen in Figure 4, Indeed, in the absence of the magnetic field, the distortions of the isotherms are observed and become more and more attenuated in the central region of the cavity by the incrementation of Ha, and at a very large value of Ha, the isotherms are almost parallel to the walls horizontals, which also subsequently causes a sharp drop in the temperature gradients on the horizontal walls of the enclosure, indicating that the convection of the fluid is dampened with the increase in the magnetic field and that most of the heat transfer in the cavity does not take place in the form of thermal convection but in the form of thermal conduction.

Figure 5 shows the effect of the Hartmann number on flux intensity and heat transfer for $Ra = 10^5$,$\theta = 0°$ and different values of n. The increase in Ha causes a very strong decrease in $|\Psi_{max}|$ and Nu, this effect becomes more pronounced for $n = 0.6$ than for $n = 1.0$ and $n = 1.4$, this is due to the increase in apparent viscosity with n, which weakens the flux intensity, where the magnetic field no longer has influence. Nevertheless, as can be seen from this figure, when Ha increases the difference between the curves relative to $n = 0.6$, $n = 1$ and $n = 1.4$ decreases, this shows that the increase in magnetic field strength suppresses the effect of rheological behavior on convective flux intensity and heat transfer.

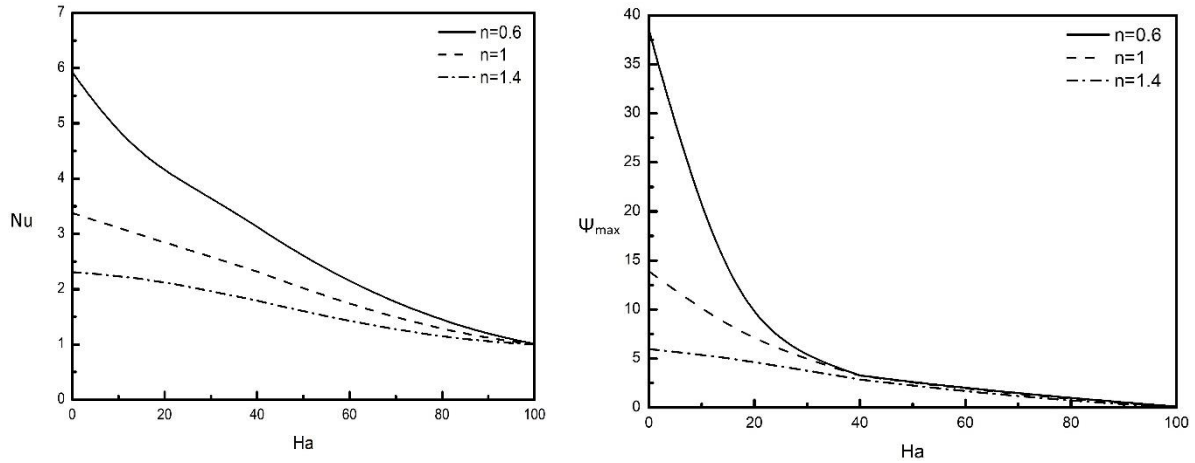

Fig. 5. Variation of the Nusselt number and the maximum of stream fonction at $Ra = 10^5$, $\Theta = 0^{\circ}$ with the variation of Hartmann number for different values of n

Figure 6 shows the distribution of velocities v in the middle of the cavity with a Rayleigh number of $Ra = 10^5$ for different power law indices and Hartmann numbers. It shows that an increase in the intensity of the magnetic field leads to a very strong decrease in the speed in the middle of the cavity, in particular, when n=0.6 instead of the behavioural fluid of index $n > 1$, because when the law index power increases, the force of resistance to viscous flow becomes stronger with respect to buoyancy, which leads to a decrease in the convection process and subsequently leads to the weakening of the magnetic force. These trends confirm the effect of the Hartmann number and the behavior index on the flow and the heat transfers already discussed. Regarding the profiles of T in the central part of the enclosure presented in Figure 7, we can also notice that these profiles become less curved with an increase in the value of n at the heart of the enclosure, the temperature are almost straight lines for high values of Ha which leads to a purely conductive regime. Moreover, it is evident that the effect of n on the temperature distributions decreases remarkably with increasing Ha.

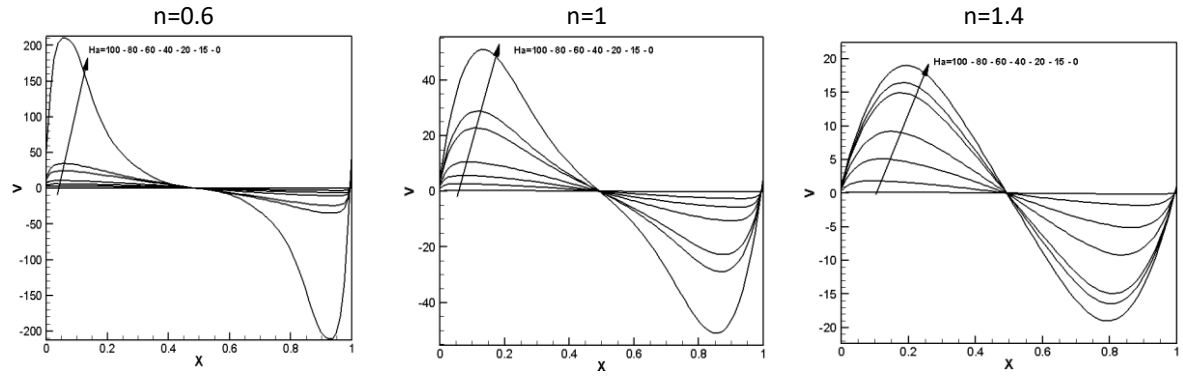

Fig. 6. Normal Velocity profile at the center of the cavity $(y = 1/2)$ for various values of the Hartman number Ha, behavior index n at $Ra = 10^5$, $\Theta = 0°$

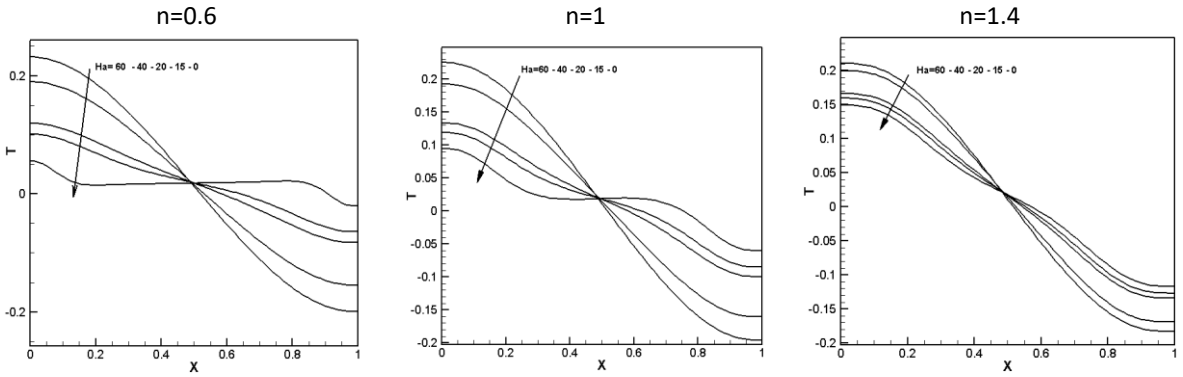

Fig. 7. Temperature at the center of the cavity $(y = 1/2)$ for various values of the Hartman number Ha, behavior index n at $Ra = 10^5$, $\Theta = 0°$

Figure 8 and Figure 9 contain the streamlines and the isotherm at $Ra = 10^5$, $Ha = 40$, and for different angles of inclination. First, one can easily notice that the distributions of the isotherms and the streamlines are almost identical in that where $\Theta = 0°$ and $\Theta = 180°$, which is proof of the periodic changes of π. It can be seen that the effect of the angles of inclination on the thermal and dynamic structure is considerable, because an elongation is very important and can be noticed in the vertical direction when $\Theta = 0°$ and separates in the horizontal direction when $\Theta = 90°$, while the flow field distributions at $\Theta = 45°$ and $\Theta = 90°$ are more complex, which mainly depends on a consequence of the competition between buoyancy and magnetic force. These phenomena are explained by the combined effect of the magnetic force and the buoyancy force. When Ha is high

enough, the flux is mainly driven by the magnetic force, which is perpendicular to the direction of the magnetic field. For example, when $\Theta = 0°$, the magnetic force acts only in the direction (y); considering the symmetry, the velocity u is dominant at the vertical centreline due to $v = 0$, which means that the total velocity is almost parallel to the magnetic field and therefore the magnetic force is close to zero, because the magnetic force can reduce the effect of buoyancy; as a result, conductive fluids are stretched larger near the horizontal axis, for the same reason, The Lorentz force acts in the horizontal direction (x) in the case where $\Theta = 90°$ or The velocities close to the horizontal walls are dominated by the vertical component of velocity v, and the horizontal component of velocity is relatively weak, which results in the dominance of the buoyancy force compared to the magnetic force which can be translated by an elongation of the cells towards the vertical walls. As a result, the streamlines on the side walls are denser (faster speed), on the contrary; the streamlines at the top and bottom of the walls are spaced out (lower speed).

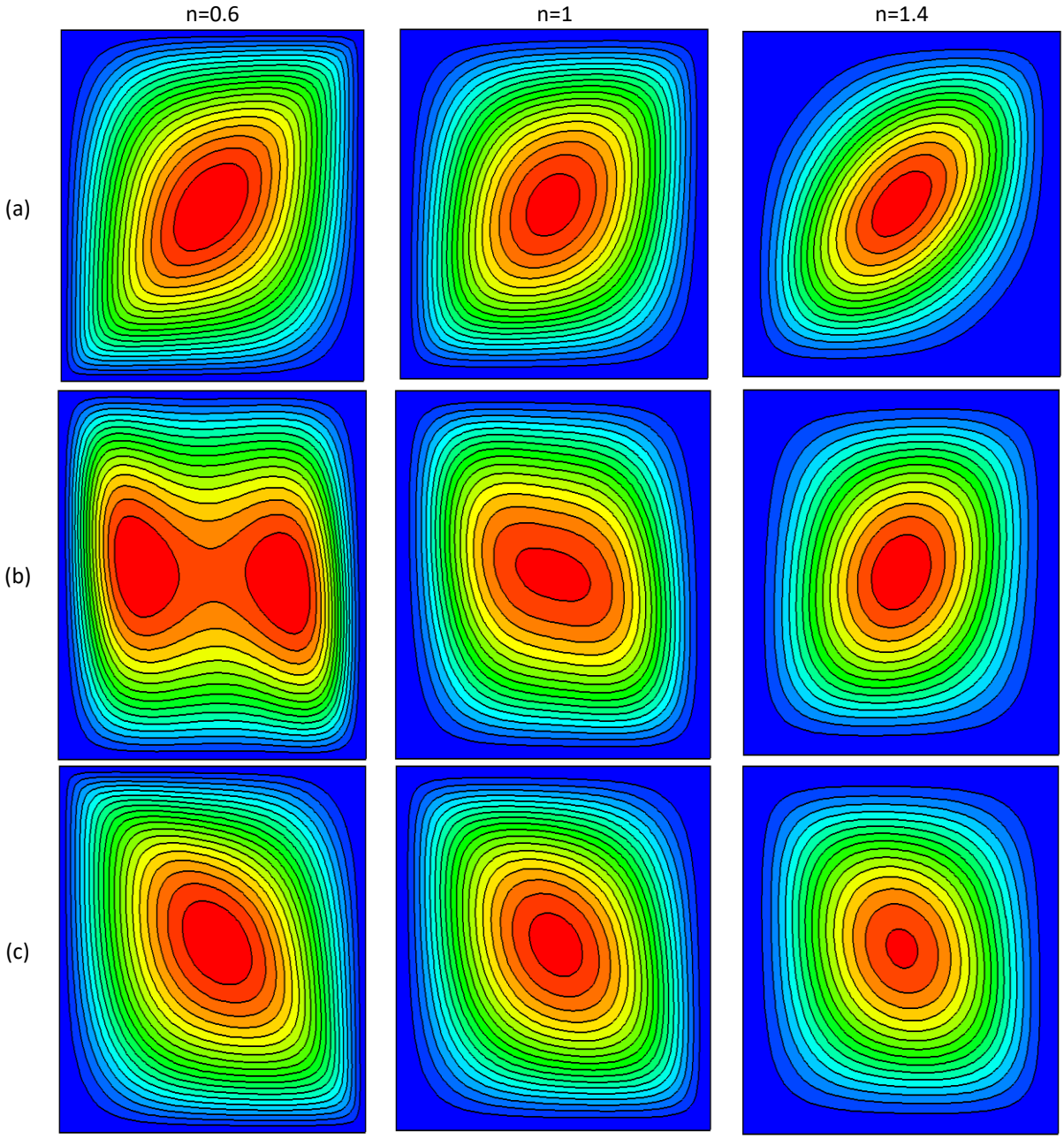

(d)

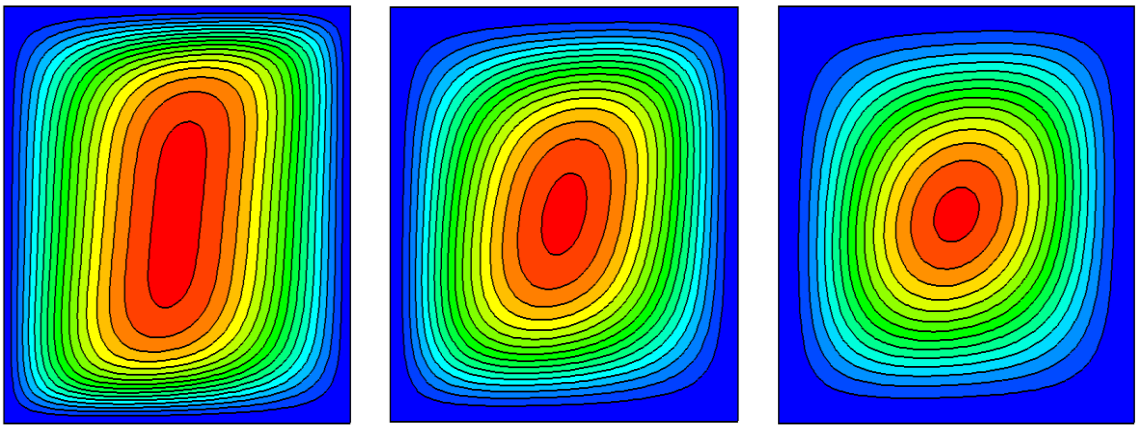

Fig. 8. Streamlines for $Ra = 10^5$, Ha=40, different values of n ((left) n =0.6, (middle) n=1, (right) n=1.4) and various values of Θ ((a) (Θ =45) 0, (b) (Θ = 90), (c) (Θ =135), (d) (Θ =180)

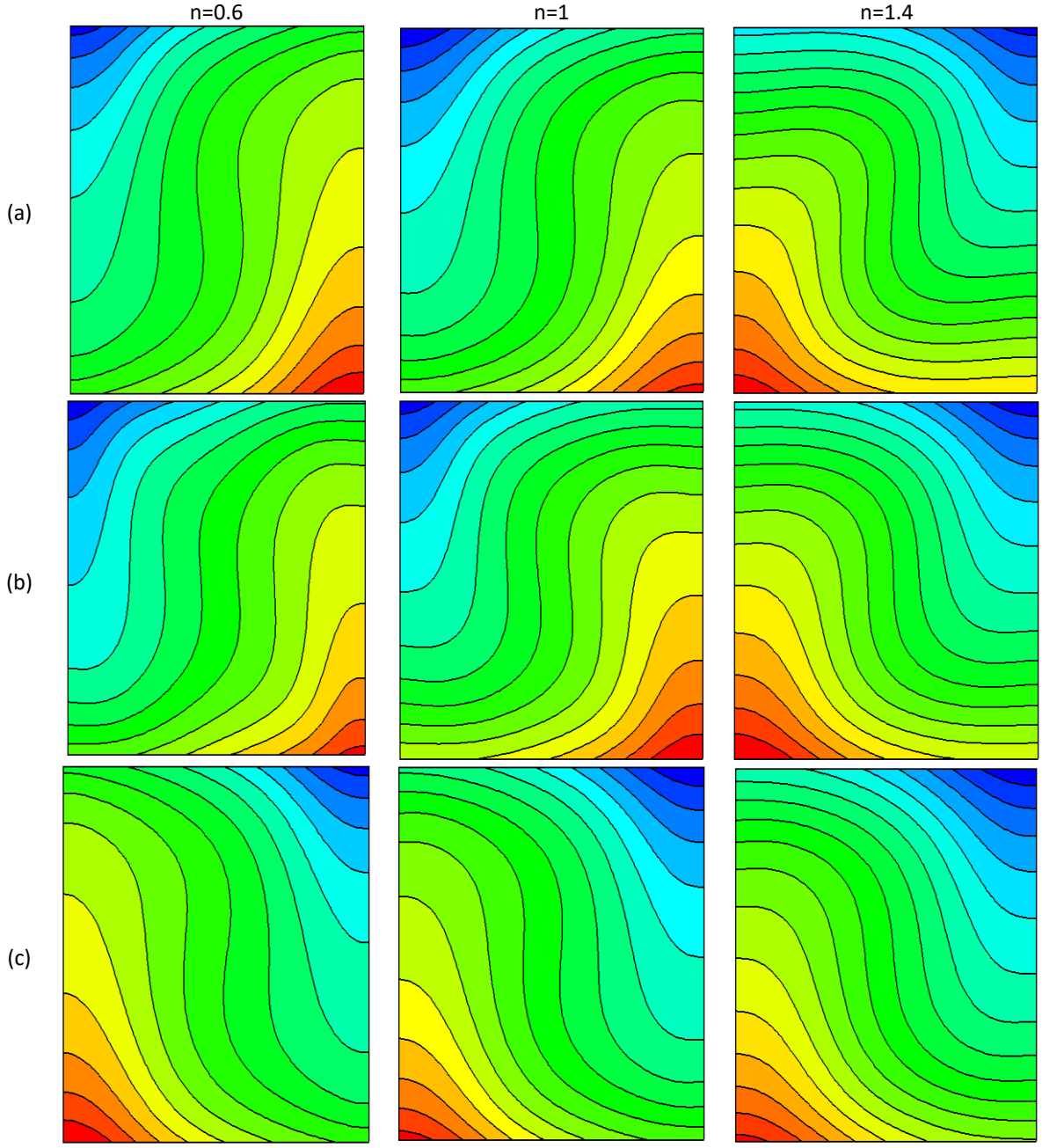

(d)

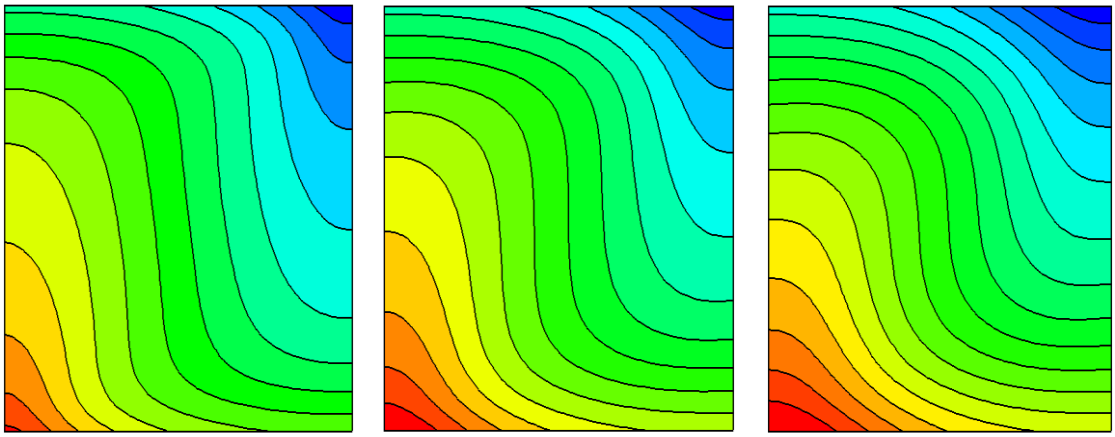

Fig. 9. Isotherms for $Ra = 10^5$, $Ha = 40$, different values of n ((left) n=0.6, (middle) n=1, (right) n=1.4 and various values of Θ ((a) ($\Theta = 45$) 0, (b) ($\Theta = 90$), (c) ($\Theta = 135$), (d) ($\Theta = 180$)

To study the influence of the directions of the magnetic field, the Nusselt number has been plotted as a function of the angle of magnetic incidence in Figure 10, under the conditions of $Ra = 10^5$ and $Ha = 40$. For a value of behavior index $n = 0.6$, we note that Nu exhibits periodic oscillations and that the Nusselt numbers reach maximums at $\Theta = 0°$, $180°$ and $360°$ and minimum values in particular around the values of $\Theta = 45°$, and $\Theta = 270°$. For the fluid of behavior index $n = 1.4$, the number of Nusselt increases monotonically with the angle of the magnetic field, which varies between $\theta = 45^{\circ}$ and $\theta = 120^{\circ}$, and for the change of angle, which varies between $\theta = 225°$ and $\theta = 315°$, then drops to a minimum value between $\theta = 120°$ and $\theta = 225°$, because the magnetic force will produce resistance in the opposite direction to the flow of fluids.

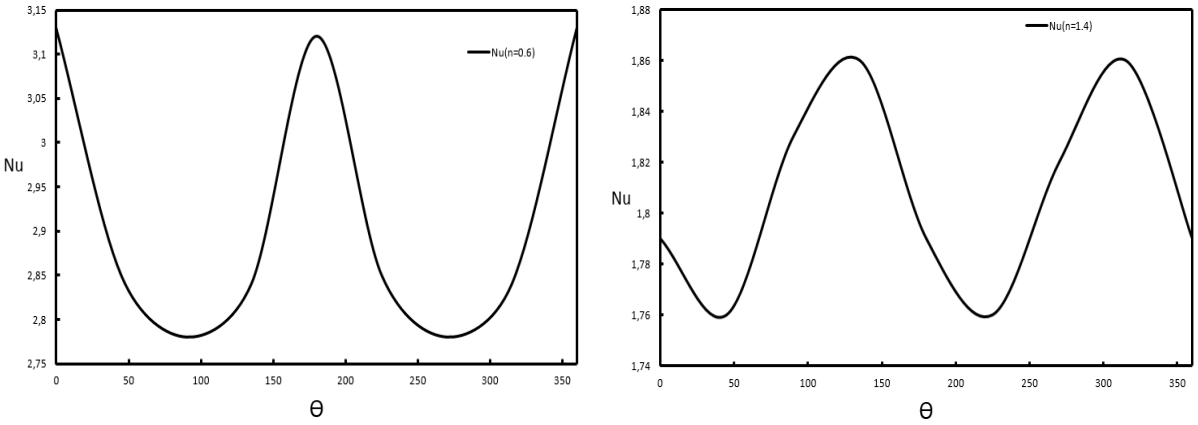

Fig. 10. Variation of Nusselt number and maximum Heat Transfer with the magnetic field inclination angle for $Ra = 10^5$, $Ha = 40$ and various values of n

Figure 11 represents the streamlines, for $Ra = 10^4$, $Ha = 35$, and for different values of the behavior index n, with and without temperature variation as a function of the viscosity. We note that when the viscosity of the fluids changes as a function of temperature, the symmetry of the convective cells begins to disappear with the increase in n, and the core of the cells migrates downwards, which leads to the formation of two zones, one stagnant, close to the horizontal wall bottom, and the other active area near the top of the horizontal wall.

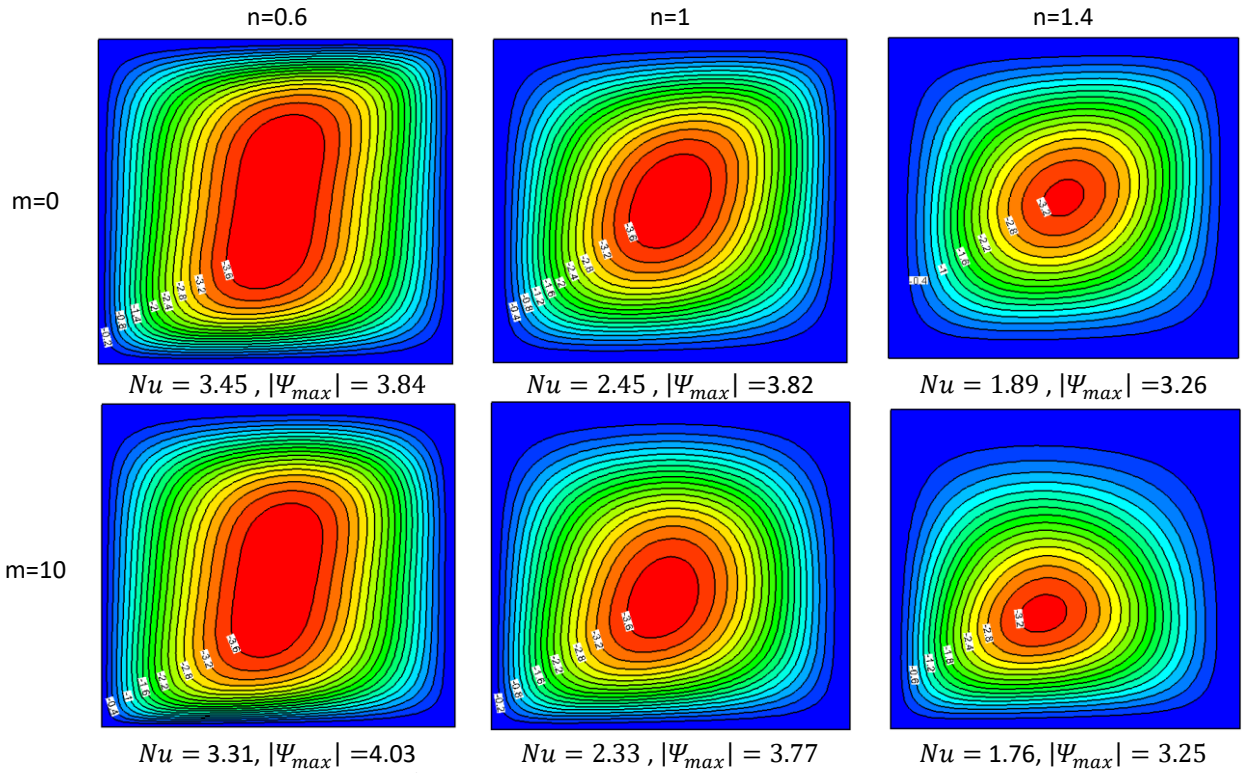

Fig. 11. Streamlines for $\mathrm{Ra} = 10^5$, $\Theta = 0^{\circ}$,for different values of n ((left) n=0.6, (middle) n=1, (right) n=1.4) and various values m and at Ha=35

Figure 12 shows the evolution of the speed according to the number of Hartmann Ha, and m, one can quickly notice that the velocity increases when the intensity of the magnetic field lacks whatever the nature between the viscosity and the temperature, which clearly shows the braking effect produced by the magnetic field. The velocity figure also shows that the rise of m causes the formation of two zones, one active near the bottom wall and the other stagnant along the top wall, due to the decrease in viscosity apparent in the active area, the elevation of m also disturbs the center symmetry of the cell which migrates towards the active zone, but in the other zone where the thermo-dependent fluid evacuates more heat, which leads to better cooling of the cavity, which pushes subsequently to the rise in the apparent viscosity, which clearly explains the weakening of the velocity in the stagnant zone.

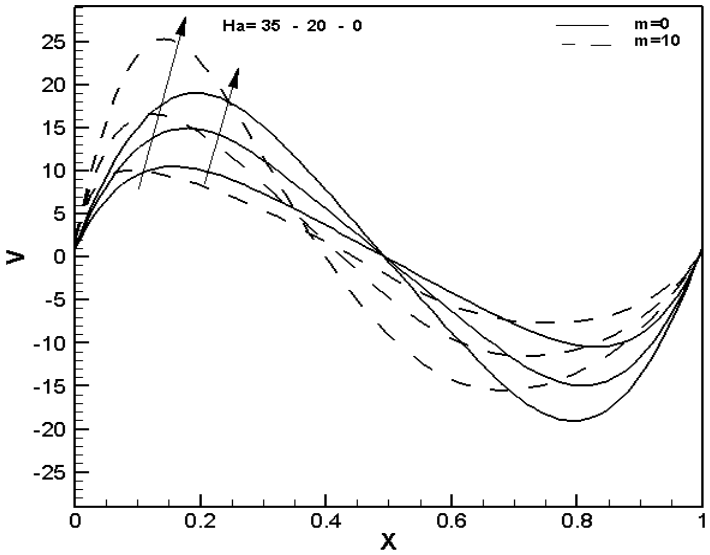

Fig. 12. Normal velocity profiles in the cavity center for various Hartman, and Pearson Numbers at $n = 1.4$ and at $Ra = 10^5$ and $\Theta = 0$

4. Conclusions

The present numerical work implements the (FVM) to study free Rayleigh Benard convection in a square cavity charged with non-Newtonian conductive fluids in the viscosity depends on the temperature, and which is subjected to an external magnetic flux. The examination of the determining parameters: the Rayleigh number Ra, the index of behavior, n, Prandtl number, Pr, Hartmann number Ha, magnetic field inclination angle, Θ, and the Pearson number, m, on the Fluid flow and heat transfer characteristics lead to the following main results:

(i) The onset of convection is controlled by the critical value Rac of the Rayleigh number, which depends on both Ha and n. This start is delayed when n and Ha increase.

(ii) The intensity of the flux and the heat transfers decrease with the improvement of the Hartmann number for Newtonian and non-Newtonian fluids, and at very high values of Ha, the convection

(iii) tends towards a conduction regime.

(iv) The improvement in the behavior index n decreases the heat transfer and the intensity of the flow, and this is due to the increase in the apparent viscosity, which leads to the slowing down of the movement of the fluid. This effect of n begins to disappear for a high Hartmann number.

(v) The orientation of the applied magnetic field has a very large effect on the heat transfer and the intensity of the flow. It is also obvious that the orientation of the magnetic field can help or oppose the buoyancy force, which leads to an elongation of the convection cells in the zones where the magnetic force cancels each other.

(vi) The dependence of viscosity on temperature for MHD leads to the formation of two zones, one active near the hot wall and the other next to the cold wall, and this tendency disappears with the weakening of the behavior index n. This phenomenon is characterized by the disappearance of the Centro symmetry of the central cell and the migration of the center toward the active wall.

Based on the findings outlined, the importance of this investigation to the scientific community lies in its valuable insights into the interactions between non-Newtonian conductive fluids, magnetic fields, and thermal conditions. These findings contribute to a deeper understanding of the complex mechanisms underlying Rayleigh-Benard convection, offering crucial guidance for the design and optimization of heat transfer systems in various industrial and engineering applications.

Acknowledgement
In order to complete this work, we are grateful to the National Centre for Scientific and Technological Research (CNRST-Morocco) for providing computer resources.

References

[1] Draper, Bridget, Win Lei Yee, Alisa Pedrana, Khin Pyone Kyi, Huma Qureshi, Hla Htay, Win Naing, Alexander J. Thompson, Margaret Hellard, and Jessica Howell. "Reducing liver disease-related deaths in the Asia-Pacific: the important role of decentralised and non-specialist led hepatitis C treatment for cirrhotic patients." *The Lancet Regional Health-Western Pacific* 20 (2022). https://doi.org/10.1016/j.lanwpc.2021.100359

[2] Alegria, Patricia, Leyre Catalan, Miguel Araiz, Antonio Rodriguez, and David Astrain. "Experimental development of a novel thermoelectric generator without moving parts to harness shallow hot dry rock fields." *Applied Thermal Engineering* 200 (2022): 117619. https://doi.org/10.1016/j.applthermaleng.2021.117619

[3] Vives, Charles, and Christian Perry. "Effects of magnetically damped convection during the controlled solidification of metals and alloys." *International Journal of Heat and Mass Transfer* 30, no. 3 (1987): 479-496. https://doi.org/10.1016/0017-9310(87)90263-8

[4] Rashidi, Saman, Javad Abolfazli Esfahani, and Mahla Maskaniyan. "Applications of magnetohydrodynamics in biological systems-a review on the numerical studies." *Journal of Magnetism and Magnetic Materials* 439 (2017): 358-372. https://doi.org/10.1016/j.jmmm.2017.05.014

[5] Al Rizeiqi, Nasser Mohammed, Nasser Al Rizeiqi, and Ali Nabavi. "Potential of Underground Hydrogen Storage in Oman." *Journal of Advanced Research in Applied Sciences and Engineering Technology* 27, no. 1 (2022): 9-31. https://doi.org/10.37934/araset.27.1.931

[6] Hussin, Norasikin, Siti Shareeda Mohd Nasir, Nor Azirah Mohd Fohimi, Rohidatun Mahmod, Yusli Yaakob, and Dzullijah Ibrahim. "Analysis of Thermal Comfort and Energy Consumption for Educational Building." *Journal of Advanced Research in Experimental Fluid Mechanics and Heat Transfer* 10, no. 1 (2022): 1-9.

[7] Sathiyamoorthy, M., and Ali Chamkha. "Effect of magnetic field on natural convection flow in a liquid gallium filled square cavity for linearly heated side wall (s)." *International Journal of Thermal Sciences* 49, no. 9 (2010): 1856-1865. https://doi.org/10.1016/j.ijthermalsci.2010.04.014

[8] Oreper, G. M., and J. Szekely. "The effect of an externally imposed magnetic field on buoyancy driven flow in a rectangular cavity." *Journal of Crystal Growth* 64, no. 3 (1983): 505-515. https://doi.org/10.1016/0022-0248(83)90335-4

[9] Pirmohammadi, Mohsen, and Majid Ghassemi. "Effect of magnetic field on convection heat transfer inside a tilted square enclosure." *International Communications in Heat and Mass Transfer* 36, no. 7 (2009): 776-780. https://doi.org/10.1016/j.icheatmasstransfer.2009.03.023

[10] Ghasemi, B., S. M. Aminossadati, and A. Raisi. "Magnetic field effect on natural convection in a nanofluid-filled square enclosure." *International Journal of Thermal Sciences* 50, no. 9 (2011): 1748-1756. https://doi.org/10.1016/j.ijthermalsci.2011.04.010

[11] Kefayati, GH. R. "Lattice Boltzmann simulation of natural convection in nanofluid-filled 2D long enclosures at presence of magnetic field." *Theoretical and Computational Fluid Dynamics* 27, no. 6 (2013): 865-883. https://doi.org/10.1007/s00162-012-0290-x

[12] Alchaar, S., P. Vasseur, and E. Bilgen. "The effect of a magnetic field on natural convection in a shallow cavity heated from below." *Chemical Engineering Communications* 134, no. 1 (1995): 195-209. https://doi.org/10.1080/00986449508936332

[13] Liao, Chuan-Chieh, Wen-Ken Li, and Chia-Ching Chu. "Analysis of heat transfer transition of thermally driven flow within a square enclosure under effects of inclined magnetic field." *International Communications in Heat and Mass Transfer* 130 (2022): 105817. https://doi.org/10.1016/j.icheatmasstransfer.2021.105817

[14] Benzema, Mahdi, Youb Khaled Benkahla, and Seif-Eddine Ouyahia. "Rayleigh-Bénard MHD convection of Al_2O_3-water nanofluid in a square enclosure: magnetic field orientation effect." *Energy Procedia* 139 (2017): 198-203. https://doi.org/10.1016/j.egypro.2017.11.196

[15] Zürner, Till, Felix Schindler, Tobias Vogt, Sven Eckert, and Jörg Schumacher. "Flow regimes of Rayleigh-Bénard convection in a vertical magnetic field." *Journal of Fluid Mechanics* 894 (2020): A21. https://doi.org/10.1017/jfm.2020.264
[16] Chtaibi, Khalid, Mohammed Hasnaoui, Youssef Dahani, and Abdelkhalek Amahmid. "Lattice Boltzmann Simulation of MHD Rayleigh-Bénard Natural Convection in a Cavity Filled With a Ferrofluid." *Journal of Atomic, Molecular, Condensed Matter & Nano Physics* 7, no. 3 (2020): 133-144. https://doi.org/10.26713/jamcnp.v7i3.1540
[17] Kefayati, GH R. "Mesoscopic simulation of magnetic field effect on natural convection of power-law fluids in a partially heated cavity." *Chemical Engineering Research and Design* 94 (2015): 337-354. https://doi.org/10.1016/j.cherd.2014.08.014
[18] Dimitrienko, Yu I., and Shuguang Li. "Numerical simulation of MHD natural convection heat transfer in a square cavity filled with Carreau fluids under magnetic fields in different directions." *Computational and Applied Mathematics* 39, no. 4 (2020): 252. https://doi.org/10.1007/s40314-020-01300-w
[19] Makayssi, T., M. Lamsaadi, and M. Kaddiri. "Numerical study of magnetic field effect on natural convection heat and mass transfers in a square enclosure containing non-Newtonian fluid and submitted to horizontal temperature and concentration gradients." *The European Physical Journal Plus* 136, no. 10 (2021): 996. https://doi.org/10.1140/epjp/s13360-021-01986-9
[20] Naffouti, Awatef, Brahim Ben-Beya, and Taieb Lili. "Three-dimensional Rayleigh-Bénard magnetoconvection: effect of the direction of the magnetic field on heat transfer and flow patterns." *Comptes Rendus Mecanique* 342, no. 12 (2014): 714-725. https://doi.org/10.1016/j.crme.2014.09.001
[21] Ahmed, T., S. Hassan, M. F. Hasan, M. M. Molla, M. A. Taher, and S. C. Saha. "Lattice boltzmann simulation of magnetic field effect on electrically conducting fluid at inclined angles in Rayleigh-Bénard convection." *Energy Engineering* (2021). https://doi.org/10.32604/EE.2020.011237
[22] Makayssi, T., M. Lamsaadi, M. Kaddiri, and Y. Tizakast. "Effect of an ascendant magnetic field on Rayleigh-Bénard convection for non-Newtonian power-law fluids in a horizontal rectangular cavity submitted to vertical temperature gradient." *The European Physical Journal Plus* 138, no. 7 (2023): 650. https://doi.org/10.1140/epjp/s13360-023-04290-w
[23] Hirayama, Osamu, and Ryuji Takaki. "Thermal convection of a fluid with temperature-dependent viscosity." *Fluid Dynamics Research* 12, no. 1 (1993): 35. https://doi.org/10.1016/0169-5983(93)90103-H
[24] Kaddiri, Mourad, Mohamed Naïmi, Abdelghani Raji, and Mohammed Hasnaoui. "Rayleigh-Bénard convection of non-Newtonian Power-law fluids with temperature-dependent viscosity." *International Scholarly Research Notices* 2012 (2012). https://doi.org/10.5402/2012/614712
[25] Patankar, Suhas V. "Numerical methods in heat transfer." In *International Heat Transfer Conference Digital Library*. Begel House Inc., 1982. https://doi.org/10.1615/IHTC7.4220
[26] Raghay, S., and A. Hakim. "Numerical simulation of White-Metzner fluid in a 4: 1 contraction." *International Journal for Numerical Methods in Fluids* 35, no. 5 (2001): 559-573. https://doi.org/10.1002/1097-0363(20010315)35:5<559::AID-FLD102>3.0.CO;2-P
[27] Van Doormaal, Jeffrey P., and George D. Raithby. "Enhancements of the SIMPLE method for predicting incompressible fluid flows." *Numerical Heat Transfer* 7, no. 2 (1984): 147-163. https://doi.org/10.1080/01495728408961817
[28] Baliga, B. R., and S. V. Patankar. "A new finite-element formulation for convection-diffusion problems." *Numerical Heat Transfer* 3, no. 4 (1980): 393-409. https://doi.org/10.1080/01495728008961767
[29] Turan, Osman, Anuj Sachdeva, Nilanjan Chakraborty, and Robert J. Poole. "Laminar natural convection of power-law fluids in a square enclosure with differentially heated side walls subjected to constant temperatures." *Journal of Non-Newtonian Fluid Mechanics* 166, no. 17-18 (2011): 1049-1063. https://doi.org/10.1016/j.jnnfm.2011.06.003
[30] Pirmohammadi, Mohsen, Majid Ghassemi, and Ghanar A. Sheikhzadeh. "The effect of a magnetic field on buoyancy-driven convection in differentially heated square cavity." In *2008 14th Symposium on Electromagnetic Launch Technology*, pp. 1-6. IEEE, 2008. https://doi.org/10.1109/ELT.2008.85
[31] Lamsaadi, M., M. Naimi, and M. Hasnaoui. "Natural convection of non-Newtonian power law fluids in a shallow horizontal rectangular cavity uniformly heated from below." *Heat and Mass Transfer* 41 (2005): 239-249. https://doi.org/10.1007/s00231-004-0530-8